1. SCIENTIFIC RESEARCH

CONDENSED MATTER PHYSICS

The main objectives of research in the framework of the theme involved the application of neutron scattering techniques and complementary methods to investigate the structure, dynamics and microscopic properties of nanosystems and novel materials, which are of great importance for the development of nanotechnologies in the fields of electronics, pharmacology, medicine, chemistry, modern condensed matter physics and interdisciplinary sciences. In the first half of 2012 until the license for the operation of the IBR-2M reactor was issued, the experimental activities conducted by the personnel of the FLNP Department of Neutron Investigations of Condensed Matter (NICM) were carried out in neutron and synchrotron centers in Russia and abroad. These activities were performed in accordance with the Topical Plan for JINR Research and International Cooperation under the existing cooperation agreements and accepted beam time application proposals. In May, 2012, the research activities on the IBR-2M reactor were resumed in accordance with the FLNP User Program. Also, the activities on the modernization of the available spectrometers and the development of new instruments were carried out in accordance with the development program plan for the IBR-2M spectrometers. Most attention was given to the realization of the top-priority projects (construction of the new DN-6 diffractometer for studying microsamples, multipurpose GRAINS reflectometer and modernization of the SKAT/EPSILON spectrometers for geophysical research).

Within the framework of investigations under the theme, the employees of the NICM Department maintained broad cooperation with many scientific organizations in Russia and abroad. The cooperation, as a rule, was documented by joint protocols or agreements. In Russia, especially active collaboration was with the thematically-close organizations, such as RRC KI, PNPI, MSU, IMP, ISSP RAS, IC RAS, and others.

A list of the main scientific topics studied by the employees of the NICM Department includes:

- Investigation of structure and properties of novel crystal materials and nanosystems by neutron diffraction;
- Investigation of magnetic colloidal systems in bulk and at interfaces;
- Investigation of structure of carbon nanomaterials;
- Magnetism of layered nanostructures;
- Investigation of nano-scale structure and functional characteristics of biological, colloidal and polymeric nanodispersed materials;
- Investigation of nanostructure and properties of lipid membranes and lipid complexes;
- Investigation of atomic dynamics of nanosystems and materials by neutron inelastic scattering;
- Investigation of texture and properties of minerals and rocks;
- Analysis of internal stresses in bulky materials and factory-made goods.

I. Scientific results.

Structure investigations of novel oxide and nanostructured materials.

The crystalline and magnetic structures of deuterated herbertsmithite $ZnCu_3(OD)_6Cl_2$ have been studied by means of neutron powder diffraction and magnetic susceptibility measurements in a wide range of temperatures (1.5-300 K) and pressures (0-10 GPa) [1]. The given compound exhibits the most ideal (among crystalline structures) realization of the 2D magnetic Kagome lattice of Cu ions with a spin s = ½ which has a ground state of a quantum spin liquid. It has been found that the application of pressure P = 2.5 GPa induces a phase transition from a quantum-disordered spin-liquid state to an antiferromagnetic ordering with the Néel temperature T_N = 6 K and magnetic elementary cell $\sqrt{3}\,a \times \sqrt{3}\,a$ (**Fig. 1**). The anomalies in the pressure behavior of Cu-O bond length and Cu-O-Cu, Cu-Cl-Cu bond angles have been revealed in the phase transition region. Possible mechanisms of these phenomena have been analyzed.

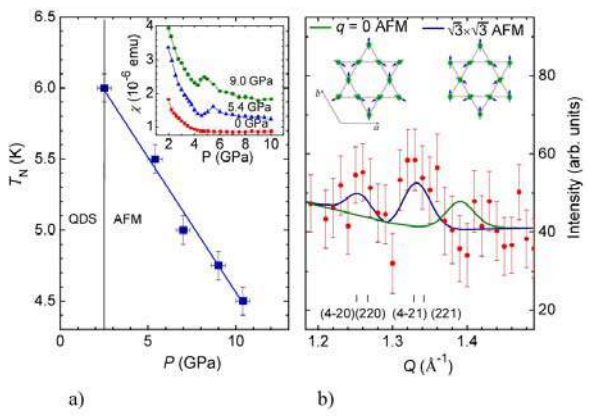

Fig. 1. a): magnetic phase diagram of herbertsmithite obtained from magnetic susceptibility measurements. b): magnetic contribution to the neutron diffraction spectrum of herbertsmithite at P = 2.7 GPa obtained by subtracting the spectrum taken at T = 50 K from the spectrum recorded at T = 1.4 K. Experimental points and model curves for two possible magnetic structures are shown.

At the HRFD diffractometer a structural phase transition in copper ferrite $CuFe_2O_4$, which is characterized by a decrease in the symmetry from a high-temperature cubic phase (*Fd*3*m*) to a tetragonal phase ($I4_1/amd$) has been studied. It has been revealed that the structural tetragonal-to-cubic phase transition (**Fig. 2**) occurs in a wide temperature range of 400 – 440°C and the equilibrium coexistence of both structural phases can be observed. The studied composition is a fully inverted spinel in a cubic phase, and the parameter of inversion in a tetragonal phase does not exceed several percent ($x = 0.06 \pm 0.04$). At the same time, the phase appeared on cooling has the classical tetragonal distortion ($\gamma \approx 1.06$). The character of the temperature changes in the structural parameters during the cubic-to-tetragonal phase transition suggests that it is based on Jahn-Teller distortions in $(Cu,Fe)O_6$ octahedrons (**Fig. 2**), but not on the boundary migration of copper and iron atoms.

Diffraction real-time *ex-situ* and *in-situ* experiments have been conducted for the first time on the HRFD diffractometer to study the structural changes that occur in chemical sources of electric current (lithium accumulators) with working substance of olivine doped with vanadium ($LiFePO_4$+xV, x = 0, 0.75%, 2% and 5%) in the course of their charging/discharging (redox-processes) in a high-resolution mode ($\Delta d/d \sim 0.001$). The ultra-low doping with vanadium makes it possible to significantly improve the properties of olivine ($LiFePO_4$) as a cathode material — electrical conductivity increases 108 times and the capacity grows by 33%. Two batteries, in one of which $LiFePO_4$ was doped with 0.75% of vanadium were studied in the *in-situ* mode in the course of charging/discharging (**Fig. 3**).

1. SCIENTIFIC RESEARCH

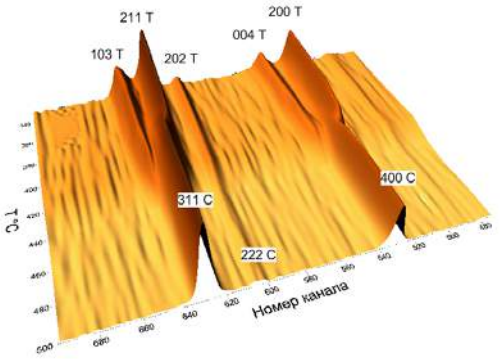

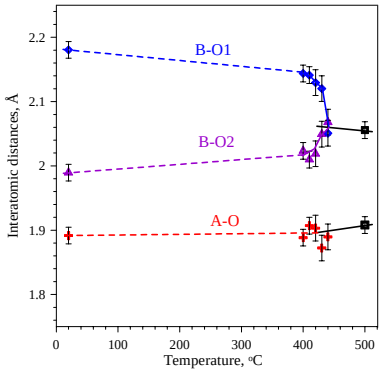

Fig. 2. Evolution of diffraction spectra of $CuFe_2O_4$ on heating from 340 to 500 °C, which evidences a structural tetragonal-to-cubic phase transition (at the top). The axis 'channel number' corresponds to interplanar distance. Miller indexes of the diffraction peaks are given with T symbol for a tetragonal phase and C symbol for a cubic phase. Dependences of interplanar cation-oxigen distances in tetrahedrons and octahedrons on temperature determined by the Rietveld method (at the bottom). In P_C phase the tetrahedrons AO_4 and octahedrons BO_6 are regular, while in P_T phase the octahedrons are stretched along the tetragonal axis (B-O1) and contracted in the perpendicular plane (B-O2).

During the charging of a battery a graphite unit cell (serves as an anode) enlarges because of the penetration of lithium ions into the structure of graphite and vice versa, diminishes down to standard sizes in the course of discharging and, correspondingly, migration of lithium ions back to a $LiFePO_4$ electrode. The enlargement and restoration of a crystal lattice of graphite, as well as the number of embedded lithium ions in Li_xC affect the position and intensity of some diffraction peaks of graphite. Phase transition $LiFePO_4 \leftrightarrow FePO_4$ was clearly observed: at $d \sim 2.4$ Å in the charged accumulator there appear two intense diffraction peaks that are characteristic for the $FePO_4$ phase. After several cycles of battery charging/discharging no degradation of the crystal structure of working electrodes was revealed.

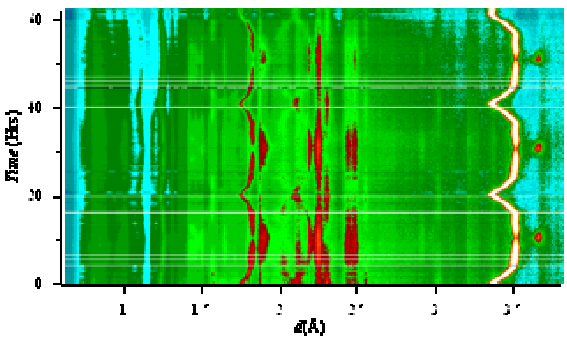

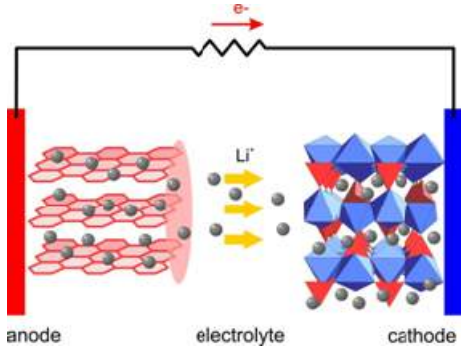

Fig. 3. At the left: evolution of neutron diffraction spectra from lithium-based electrical current source in the process of three charging/discharging cycles. Each full charging/discharging cycle takes about 20 hours. An intense peak at $d \approx 3.5$ Å is from graphite anode; peaks in the region of 2 - 2.5 Å are from olivine. At the right: illustration of the lithium ion migration during a charging/discharging cycle for a $LiFePO_4$-based Li-ion battery (cathode is at the right). During the charging process lithium ions are intercalated into the graphite lattice making it to expand; and vice versa, during the discharging process lithium ions leave the graphite lattice and its standard structural parameters are restored. From *Janina Molenda and Marcin Molenda (2011).*

The features of the crystalline structure of crystallophospors $Lu_3Al_5O_{12}:Ce^{3+}$ produced by the colloidal chemical method have been investigated by means of neutron diffraction at room temperature and the influence of the peculiarities of high-temperature annealing on the crystalline structure and spectral luminescent properties of the samples have been studied. The results of the research show that at a certain annealing temperature the growth of the interatomic bonds of oxygen octahedrons slows down as well as the intensity of luminescence. It is suggested that this effect is related to the peculiarities of the formation of a defect structure in $Lu_3Al_5O_{12}:Ce^{3+}$ and probable precipitation of cerium in other crystallographic positions different from those of lutetium Lu. This fact is confirmed by the appearance of additional peaks in the luminescence spectra, which are due to the occurrence of new channels of optical relaxation.

The effect of the synthesis conditions on the structure and sorption properties of titanium-based nanosorbents has been studied (**Fig. 4**). The morphology of the synthesized nanosorbents has been determined using scanning electron microscopy. The crystalline structure and sorption properties have been found by X-ray powder diffraction.

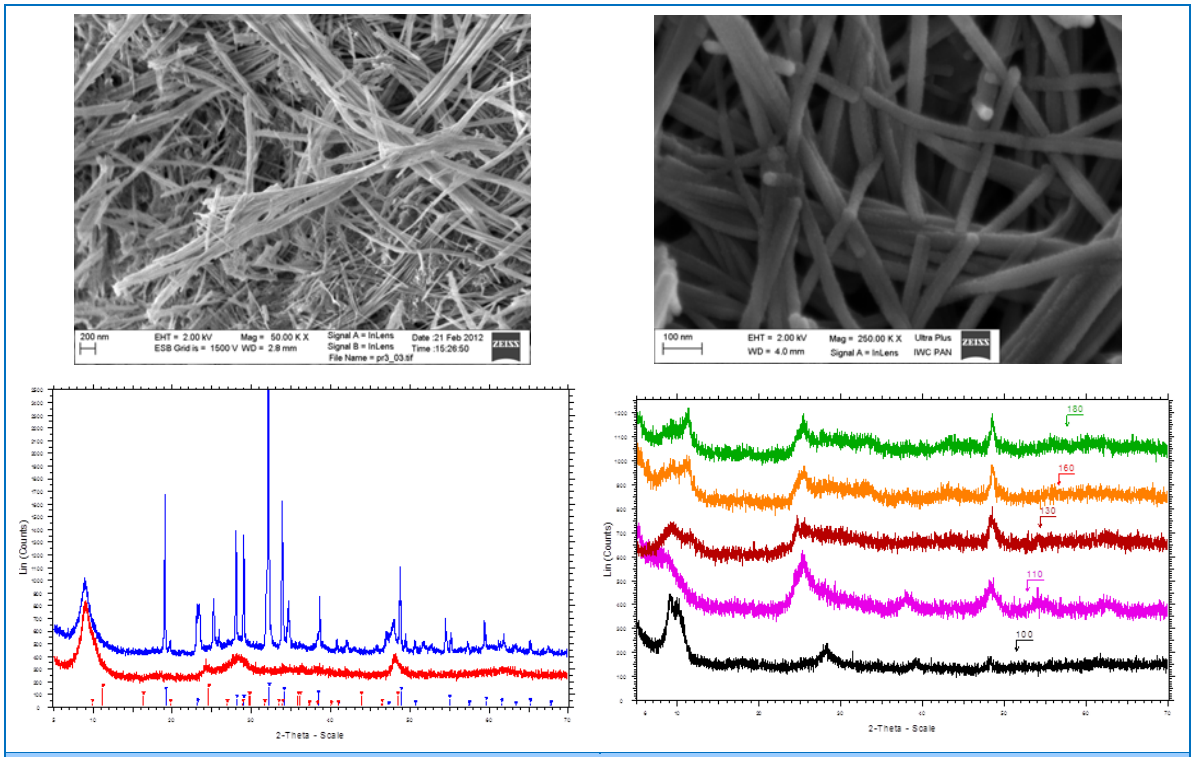

Fig. 4. At the top: nanosorbents based on $TiOSO_4$, temperature of synthesis 120°C (at the left), and TiO_2, temperature of synthesis 120°C (at the right). At the bottom: diffraction patterns from nanosorbent (blue line – nanosorbent after synthesis of $TiOSO_4$ with NaOH in ethanol at a temperature of 120°C), (red line – nanosorbent after washing with water) – at the left. Diffraction patterns from nanosorbents synthesized at various temperatures, after sorption of cesium – at the right.

1. SCIENTIFIC RESEARCH

Investigation of magnetic fluids and nanoparticles.

Small-angle neutron scattering has been applied for studying solutions of magnetoferritin—artificial biological complex on the basis of apoferritin in whose cavity the synthesis of iron oxides is initiated by chemical methods. By means of the contrast variation method the mean scattering length density of magnetoferritin and its relative composition have been determined depending on the loading factor LF, which is the mean number of iron atoms per one apoferritin complex. The measurements have revealed a significant shift in the match point of magnetoferritin with increasing LF, which is probably related to a partial distortion of the apoferritin shell (**Fig. 5**) [2].

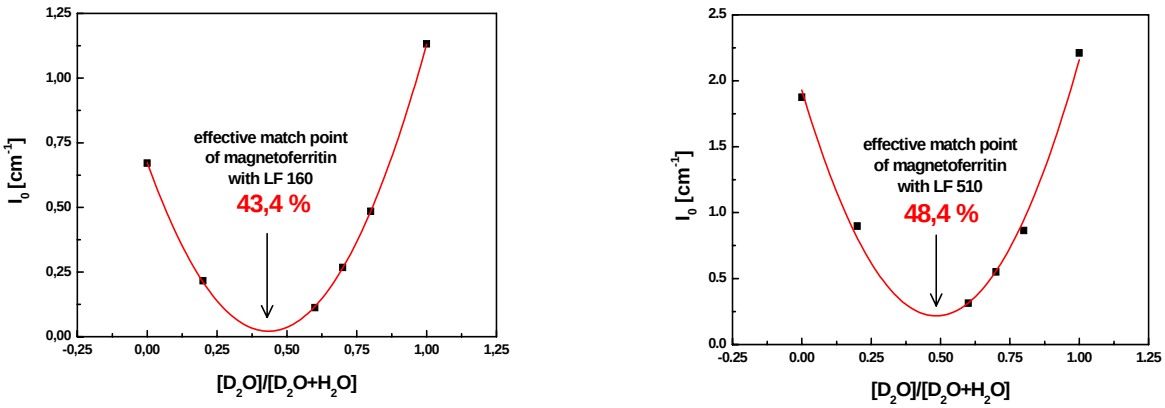

Fig. 5. Dependence of forward SANS intensity (YuMO, IBR-2M) on the relative content of deuterated component in the mixture D_2O/H_2O for solutions of magnetoferritin at two values of the loading factor LF. The arrows denote the match points.

The structural parameters of various components of magnetic fluids based on decaline with an excess of surfactant (oleic acid) have been obtained basing on the data of small-angle neutron scattering (instruments Yellow Submarine of the Budapest Neutron Center and SANS-II of the Paul Scherrer Institute). It has been shown that the structural changes concern mainly the character of the interaction between free surfactant molecules in the bulk of the magnetic fluids. However, an increase in the attraction between the surfactant molecules in the presence of magnetic particles is significantly less in decaline than in the analogous systems based on benzene. This correlates with the fact that, in contrast to benzene, decaline-based magnetic fluids remain aggregatively stable in a range of the surfactant excess up to 25 vol. %. Thus, from the microstructural viewpoint the solute-surfactant interaction plays a significant role in the stabilization of the given systems at the surfactant excess.

The experiments on neutron reflectometry (reflectometer with horizontal sample plane NREX, reactor FRM-II, Munich) have been carried out to study the structural organization of nanoparticles of two magnetic fluids at the interface with crystalline silicon. The effect of the introduction of biocompatible polymer (polyethyleneglycol) into the particle composition of the initial electrostatically stabilized magnetic fluid (magnetite coated with sodium oleate in water) has been investigated.

At the first stage of the complex investigation of the effect of magnetic nanoparticles on the conformation of amyloids the structure analysis of amyloidal fibrils of hen egg white lyzosyme stabilized in acidic medium has been carried out using small-angle neutron (SANS) and small-angle X-ray (SAXS) scattering from aqueous solutions, as well as by atomic force microscopy with the

adsorption of fibrils on a mica surface [3]. It has been shown that the obtained small-angle scattering curves (**Fig. 6**) are consistent with the helical structure of protofilaments forming amyloidal fibrils. For the analysis a simple approximation has been proposed, which makes it possible to find out the period of repetition (pitch) and the mean diameter of the helix, as well as the effective radius of their basic structural units. Some kind of 'isotope effect' on the helical structure was observed when using a heavy component in the solvent (H_2O/D_2O mixtures), which showed a significant increase in the helix diameter for the solutions with the dominant fraction of D_2O.

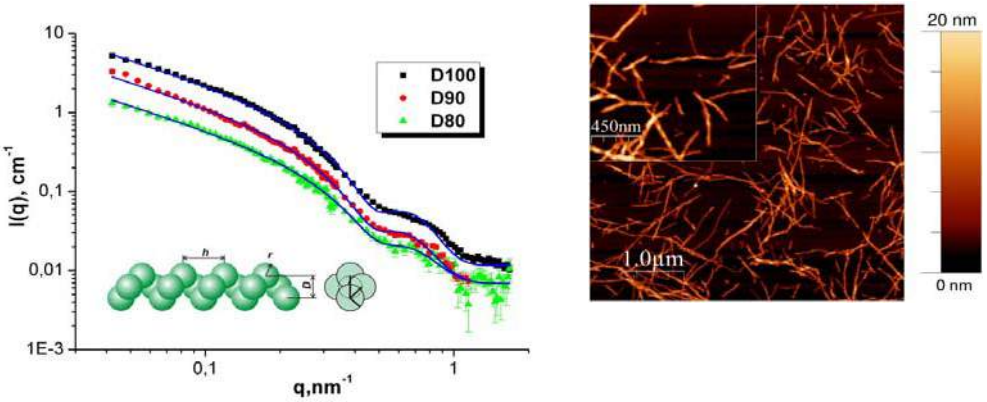

Fig. 6. Small-angle neutron scattering curves (SANS-II, PSI) from fibril amyloidal aggregates of hen egg white lyzosyme at different content of D_2O in solution. The curves are approached by the model 'helix from homogeneous spheres' whose parameters are illustrated in the inset. At the right the AFM image (IEP SAS) is shown for analogous aggregates adsorbed on the mica surface from D_2O.

Investigation of carbon nanomaterials.

The theoretical description of the kinetic growth of clusters in C_{60}/NMP and other polar solutions continued [4]. For the two models of fullerene aggregation proposed previously the time extrapolation of numerical solutions for kinetic equations has been performed. This has made it possible for the first time to obtain stationary size distribution functions of the clusters, *f(n)*, for the final stages of the cluster growth (**Fig. 7**). For one of the two models the stationary functions are well described by the so-called Slezov's functions for the classical coalescence. For another model it has been shown that among simple distribution functions the lognormal distribution gives the best fits. The calculations of *f(n)* have been made for different model parameters τ and τ_c corresponding to characteristic relaxation times in the solution.

The calculations of the evolution of the SANS curves have been made for different models of the cluster growth in C_{60}/NMP solution (**Fig. 7**). In the case of the model where the C_{60}-NMP complex formation is considered as a transition of fullerene molecules into the state of an oversaturated solution one can see that the shape of the SANS curves is inconsistent with the experimental data. This result is determined by the low polydispersity of *f(n)*, which can be explained by the error in the extrapolation (in the case of the second model this error is significant, since even the lognormal distribution poorly describes the distribution functions). The work has been done in cooperation with the University of Ulan-Bator (Mongolia).

1. SCIENTIFIC RESEARCH

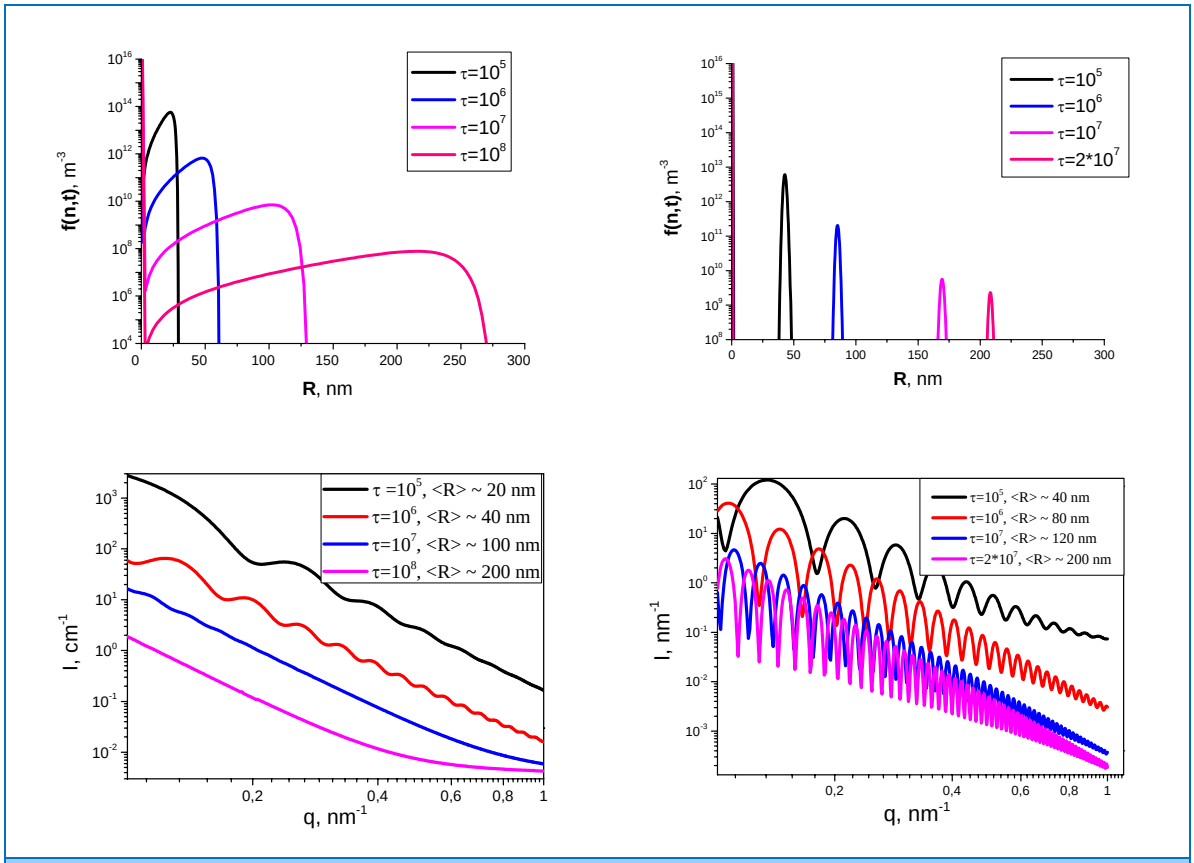

Fig. 7. At the top: stationary size distribution functions for fullerene clusters in solution C_{60}/NMP obtained by the extrapolation method for kinetic equations for two different models and various values of parameters τ and τ_c. The order of magnitude of τ-values corresponds to real times of the cluster growth. At the bottom: SANS curves calculated for the model stationary functions f(n) of the C_{60}/NMP solution at various parameters τ and τ_c.

Also, the experimental investigations of the properties of C_{60} solutions in mixed solvents continued. Thus, for the mixed solution C_{60}/NMP/toluene a non-reversible solvatochromic effect has been observed. It manifested a significant difference in the behavior of the absorption spectra of visible and ultraviolet range depending on the relative composition of the solvent for different ways of the solution preparation. If on addition of NMP into the initial solution C_{60}/toluene one can speak about classical solvatochromism (proportional shift of characteristic absorption peaks), in the reverse case, when toluene is added into the initial solution C_{60}/NMP, the selective solvatochromism is observed; toluene starts to penetrate the solvate shell only at its very high (> 95%) content in the solvent bulk. This behavior is related to a strong difference in the dielectric properties of the two types of the solvent molecules. An important observation of the research was that the found effect depends on the age of the initial solution and is influenced by the cluster state in C_{60}/NMP.

Investigation of magnetic nanostructures.

The transmission of non-polarized neutrons through a non-complanar structure has been investigated to reveal its dependence on the sequence order of magnetization components in the path of neutron wave propagation. Neutrons were reflected from two mirrors with the magnetizations

perpendicular to each other and lying in the reflection plane of the mirrors. The magnetic field was directed perpendicular to magnetization vectors. The coefficients of successive neutron reflections from the two mirrors in two cases of the opposite directions of the magnetic field are shown in **Fig. 8** together with their relative difference. The amplitude of the oscillations of this difference corresponds to the neutron polarization of 0.2-0.25 in the reflected beam. The period of oscillations of 0.7 Å corresponds to the period of Larmor precession in a magnetic field of 27 Oe. Thus, it has been experimentally shown that the polarized neutron beam transmission for non-complanar structures depends on the mutual orientation of three magnetic moments.

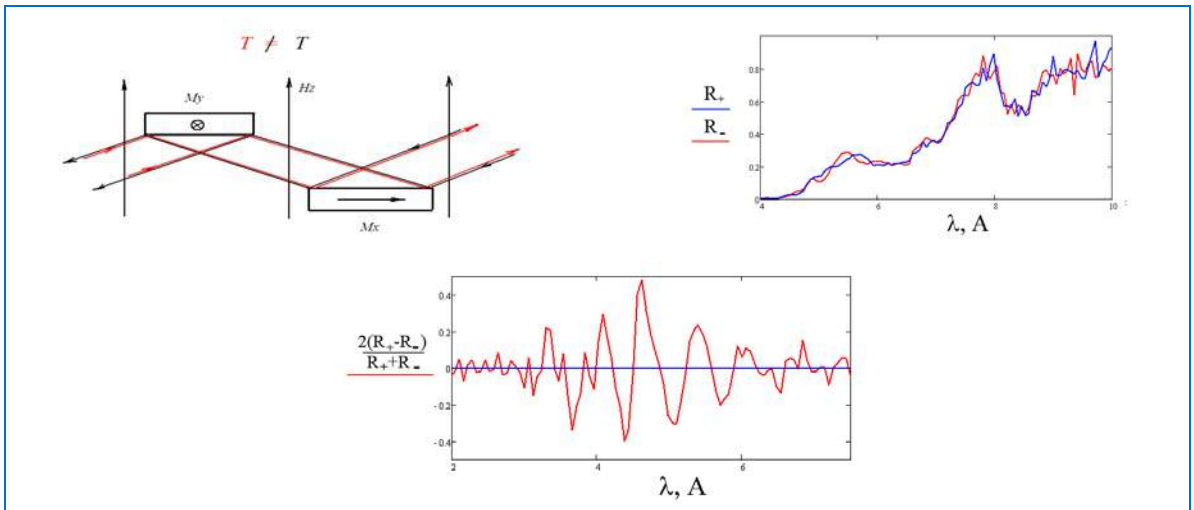

Fig. 8 Scheme of the experiment (upper panel). The coefficient of reflection from two neutron mirrors polarized perpendicular to the planes of the mirrors in a magnetic field of 27.5 Oe (blue line) and -27.5 Oe (red line) and relative difference of the coefficients of double reflection depending on the neutron wavelength (middle and lower panels).

Investigation of biological nanosystems, lipid membranes and lipid complexes.

The formation of micelles of photosensitive surfactant azobenzene trimethylammonium bromide (AzoTAB) has been studied by means of small-angle neutron scattering. In the trans-conformation the AzoTAB molecule forms charged ellipsoidal micelles. The micelle size and aggregation number increase with growing AzoTAB concentration. The temperature increase results in a decrease in these parameters. In contrast, the degree of dissociation of bromine ξ drops when the AzoTAB concentration increases and rises with increasing temperature. Under the ultraviolet irradiation the shape of the scattering curves changes sharply in the covered range of the momentum transfer q, which is indicative of reorganization of AzoTAB aggregates. It is possible that in this case AzoTAB forms strongly anisotropic objects. It has been shown that the addition of the photosensitive surfactant to nucleic acids causes their compaction. Along with this the compaction effect is also photosensitive. It is explained by the change in the surfactant conformation depending on the irradiation wavelength. Thus, the irradiation of the system by ultraviolet light causes the transition of the AzoTAB molecule from trans- to cys-conformation, which promotes the isolation of AzoTAB from RNA/DNA and decompaction of polynucleotide chains.

1. SCIENTIFIC RESEARCH

The investigations of the phase transition from the liquid crystal phase to the ripple-phase in aqueous solutions of lipid membranes DPPC/D_2O have been carried out using small-angle neutron scattering and simultaneous volumetric P-V-T measurements (**Fig. 9**). The thickness of the lipid bilayer (using SANS data) and changes in its volume (using volumetric data) have been determined. The achieved high precision in the determination of the volume changes made it possible to estimate the changes in the lipid molecule area as a result of the phase transition, which was found to be 6 $Å^2$ in agreement with the results of other works.

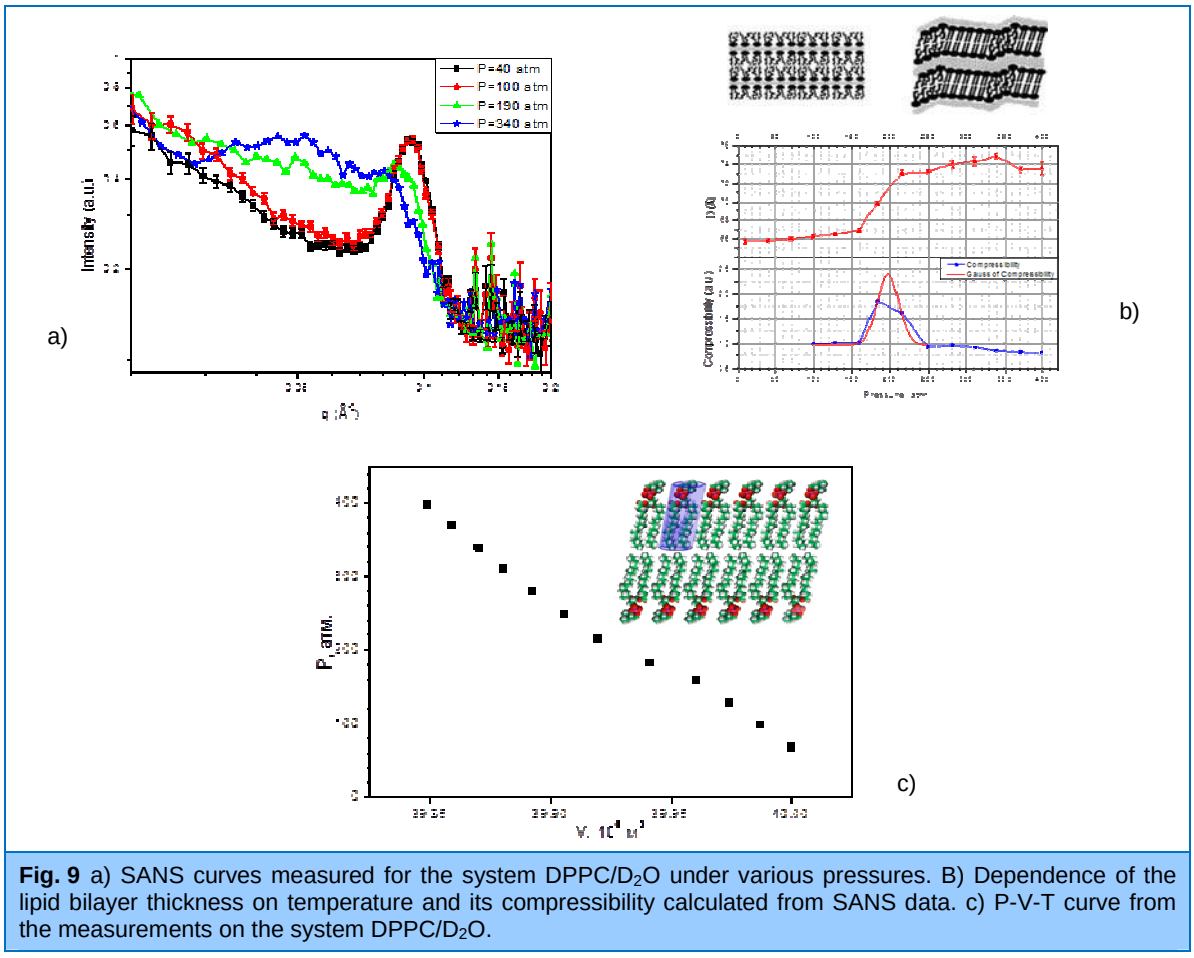

Fig. 9 a) SANS curves measured for the system DPPC/D_2O under various pressures. B) Dependence of the lipid bilayer thickness on temperature and its compressibility calculated from SANS data. c) P-V-T curve from the measurements on the system DPPC/D_2O.

The effect of salt on the structure of lipid membranes has been studied using the DMPC/H_2O/CaCl system as an example. It has been shown that with increasing concentration of calcium ions the multilamellar membranes undergo a transition to an unbound state in both gel and liquid-crystal phases. The obtained results are indicative of continuous (non-abrupt) character of the transition. The rise of the small-angle part of the curves with increasing concentration is also evidence in favor of this hypothesis. The analysis of small-angle scattering curves for multilamellar DMPC membranes has demonstrated that the destruction of the lamellar structure and the formation of single-layer vesicles occur at C_{Ca2+} ~ 0.3 mM in $L_{\beta'}$ phase and at C_{Ca2+} ~ 0.4 mM in L_{α} phase. The C_{Ca2+} values depend on both the phase state of the system and the concentration of the lipid. The detailed analysis of the diffraction peaks has made it possible to refine the numerical values for the

concentration of Ca2+ ions necessary for the bound-to-unbound transition of the system under study. It has been shown that in the pre-transition region the reduction of the lipid concentration does not affect the repeat distance in lipid membranes. The thicknesses of lipid bilayers formed spontaneously of multilamellar membranes in the region of the system transition to an unbound state correspond to the thicknesses of single-layer vesicles prepared by the extrusion method. This is direct evidence that single-layer vesicles are formed following the collapse of the lamellar phase of multilamellar DMPC membranes in both gel and liquid-crystal phases. Further addition of calcium ions results in partial adhesion of single vesicles.

Multilamellar membranes of DPPC (1,2-dipalmitoyl-sn-glycero-3-phosphatidylcholine) and mixture DPPC/POPC (1-palmitoyl-2-oleylphosphatidylcholine) in excess of water have been investigated by small-angle X-ray scattering and neutron small-angle scattering. The structural parameters of lipid bilayers have been determined in a temperature range of 3-60°C. It has been shown that the addition of POPC to DPPC/H_2O does not change the temperature of the DPPC main phase transition within the limits of experimental error. The observed phase separation occurs for the system DPPC/POPC/H_2O up to the pre-transition temperature (gel phase - ripple phase) of the DPPC multilamellar membranes. It has been found that the repeat distance of the gel phase for the DPPC/POPC mixture is smaller than that for DPPC. This effect is more pronounced for the samples measured by SAXS.

Model lipid membranes modeling the lipid component in the mucous membranes of the oral cavity of mammals based on ceramide-6 have been investigated by means of neutron diffraction (**Fig. 10**).

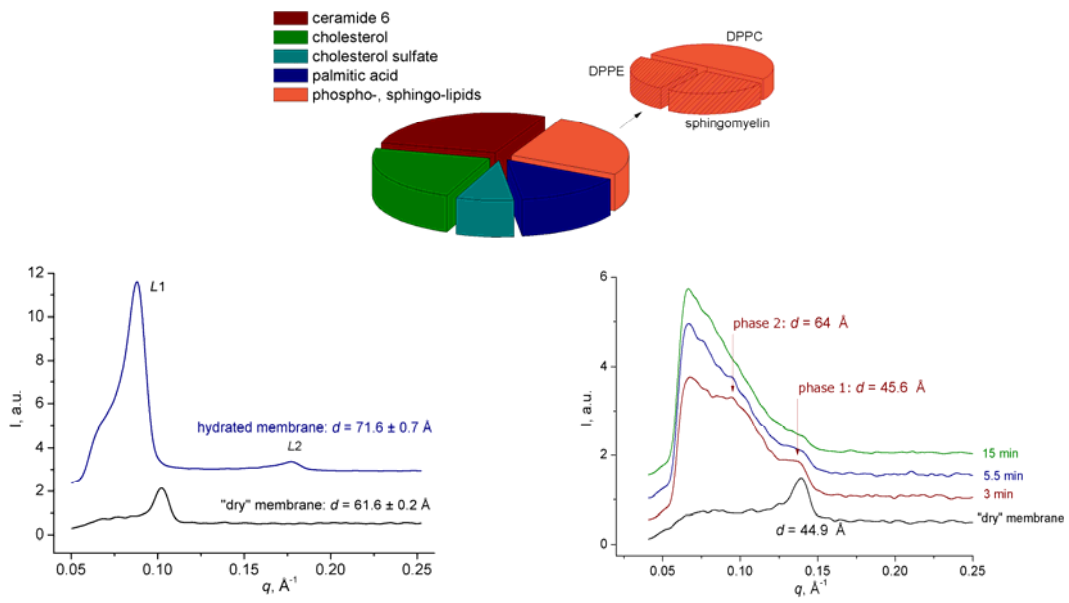

Fig. 10. At the top: composition of model OSC lipid membranes. At the bottom: diffraction spectra from model membrane DPPE/DPPC/SM in dry and hydrated states. The membrane is fully hydrated within 2 minutes after it is placed in the cell with water (at the left). Diffraction spectra from model OSC membrane = cer6/chol/PA/cholS/PL = 28/23/15/8/26 (PL= DPPE/DPPC/SM) in the process of hydration (at the right).

1. SCIENTIFIC RESEARCH

It has previously been shown that the model oral stratum corneum (OSC) membrane composed of ceramide-6/cholesterol/cholesterol sulphate/palmitic acid/DPPC/DPPE/ sphingomyelin at 37°C and a relative humidity of 99 % is characterized by the co-existence of several structural phases with repeat distances of 55, 46 and 58 Å. The experiments performed with oriented samples in excess of water have revealed that one of the structural phases shows the behavior similar to that of the model stratum corneum membrane with a slight increase in the repeat distance during the first several minutes of hydration from 44.9 to 45.6 Å. Since it is generally recognized that low hydration in SC is mainly due to ceramides, the data allow us to suggest that there are ceramide-richdomains in the lipid component of the natural mucous membrane, which are responsible for permeability control.

The morphology of the mixed double systems of DPPC/sodium cholate (basis of transdermal vesicular drug carriers) has been studied by the small-angle neutron scattering technique. It has been shown that in a temperature range of 10-60°C a lamellar-to-micellar phase transition occurs at 15°C, in a temperature range of 15-25°C the system exists in the micellar phase and at a temperature of 25°C undergoes a transition to the lamellar phase It has been suggested that the reason for this unusual temperature dependence of the double system of DPPC/sodium cholate is the existence of a minimum in the critical micelle concentration of sodium cholate in a temperature range of 15-25°C.

Atomic and molecular dynamics.

The quantum-chemical calculations of the lattice dynamics of vanadium oxide in polymorphic phases α-V_2O_5 and β-V_2O_5 have been performed [5]. Vanadium oxides are widely used in thin film electrochemical devices and as cathodes of lithium batteries due to their high energy density and retention capacity upon cycling. The model vibrational spectra showed satisfactory agreement with the experimental Raman spectra. Their analysis permitted a reliable description of all observed spectral features, and made it possible for the first time to establish 'structure-spectra' relationship for the two polymorphs of vanadium pentoxides. The activation energy of the phase transition α-$V_2O_5 \rightarrow \beta$-V_2O_5 has been estimated together with the additional calculations aimed at revealing possible mechanisms of the transition.

The neutron dynamic experiment on liquid sodium (T = 105-420°C) and sodium-hydrogen melt (T = 420°C, hydrogen concentration C ~ 0.04 % at.) has been carried out. It has been established that hydrogen is present and diffuses in the melt in the form of sodium hydride NaH. Basing on the analysis of the widths of the quasi-elastic scattering peaks (**Fig. 11**) the information on the diffusion properties of the matter has been obtained.

The temperature dependence of the phonon density of states has been studied for the most refractory metal – tungsten – which is of current interest for reactor applications. For the first time, the vibration spectrum of the crystalline lattice at temperatures of 293 and 2400 K has been obtained in the direct experiment. The vibration spectrum at a temperature of 2400 K is shifted towards lower frequencies because of the effect of the anharmonicity of vibrations. Along with this, the main peculiarities of the detailed structure characterizing BCC lattice remain unchanged.

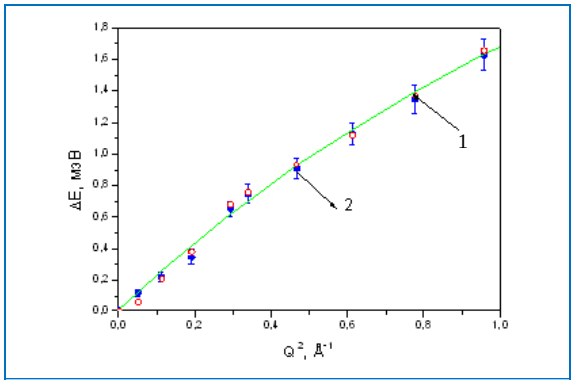

Fig. 11. FWHM of peaks of quasielastic neutron scattering from pure sodium (1) and sodium-hydrogen melt (2) for a temperature of 420°C. The curve corresponds to the model of mixed diffusion.

Applied research.

Among traditional applied investigations in the NICM Department are the experimental studies of internal stresses and texture of rocks and minerals, determination of internal stresses in bulk materials and products, including engineering materials and components of machines and devices. For the most part, these investigations are carried out using neutron diffraction.

A new comprehensive approach to the study of physical properties of layered textured rocks has been realized. It is based on the fabrication of model samples with specified characteristics, which are close in their internal structure and crystallographic texture to the real objects formed under natural conditions of the Earth's lithosphere. For this purpose the velocities of quasi-longitudinal elastic waves propagating through two-phase layered model samples in the shape of a ball made of mineral powder fillers (muscovite, quartz) and binding layered epoxide have been measured (**Fig. 12**). It has been revealed that samples with muscovite and quartz fillers have different relations between the layered structure and the spatial distribution of the velocities of quasi-longitudinal elastic waves, which is due to the process of fabrication of the models (deposition) [6].

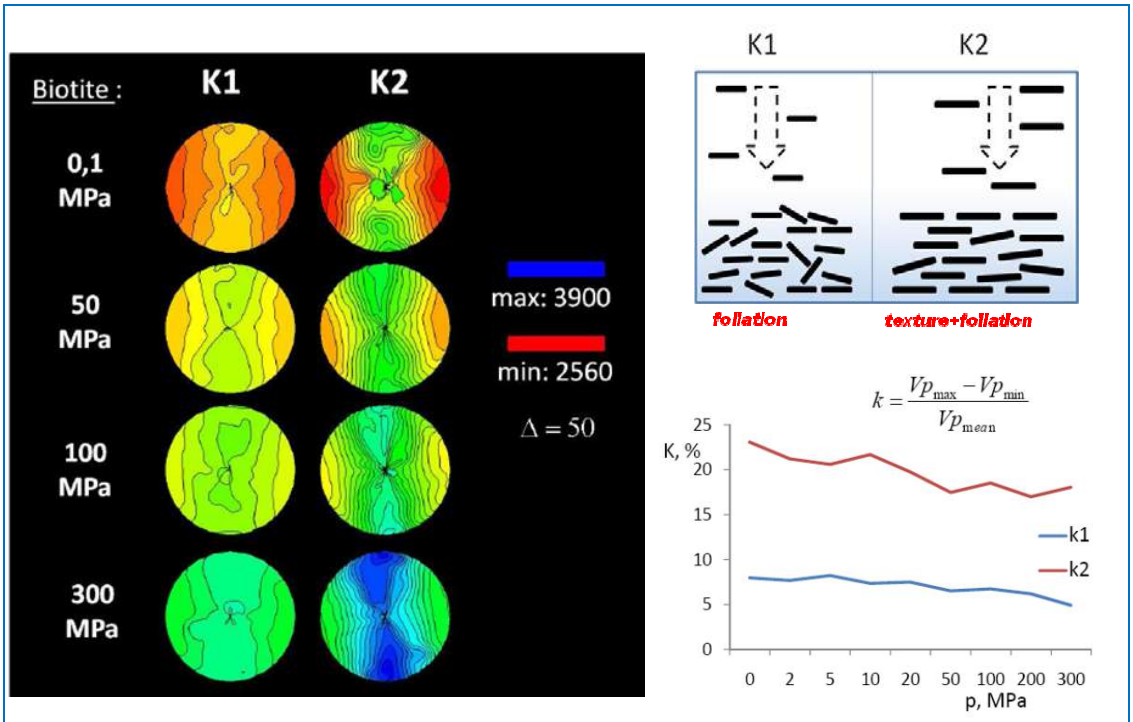

Fig. 12. Spatial distribution of the velocities of longitudinal elastic waves for model samples K1 and K2.

In collaboration with the State Center for Machine-Building Technology (TSNIITMASH) the processes of formation and decomposition of martensite after normalizing at 1050°C and further annealing in a temperature range of 500-840°C have been studied for heat-resistant ferritic-martensitic steels 10Х9К3В2МФБР and P91 (Russian notation). These steels are very promising materials for thermal and nuclear power engineering because they can be employed in power facilities at temperatures up to 650°C and vapor pressures up to 35 Pa, and their radiation resistance may amount to as much as 200 dpa.A strong anisotropy of the diffraction peak width (**Fig. 13**) caused by a

high dislocation density (as a result of martensite transition) was observed; the values of microdeformations and the dislocation density, as well as their decrease with increasing temperature and annealing time, were determined. The measured SANS spectra showed the strong surface fractal scattering in these martensites. At the annealing temperature of 600°C the intense precipitation of fractal particles of carbides and nitrides was observed during 1 hour. At further annealing the carbides were aggregated up to sizes out of the limits of the SANS method. At the same time the scattering from surface fractals reappeared up to the highest annealing temperatures.

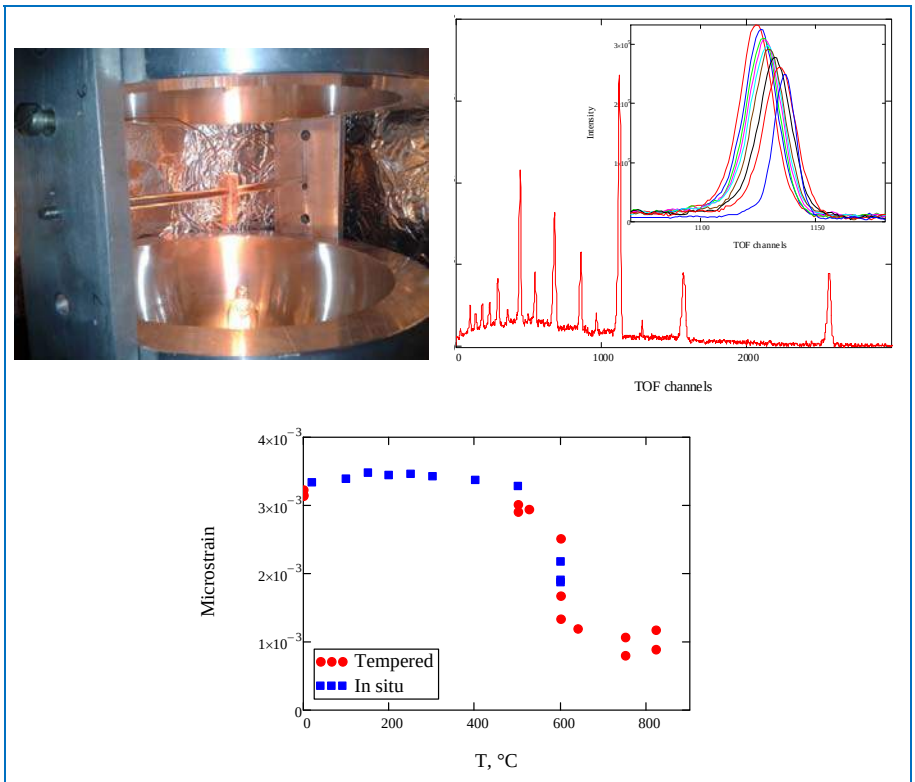

Fig. 13. At the top: sample of heat-resistant ferritic-martensitic steel 10Х9К3В2МФБР (Russian notation) at FSD at T=600 °C (at the left). Spectrum of steel 10Х9К3В2МФБР with characteristically widened diffraction peaks. The inset shows changes in the position and shape of the diffraction peak (211) with increasing temperature (at the right). At the bottom: Relaxation of microstrains in steel 10Х9К3В2МФБР with increasing annealing temperature.

The measurements of the local texture in a number of samples based on magnesium alloy MA21 (produced by intensive plastic deformation according to the technology of equal-channel angular pressing ECAP) have been carried out by means of synchrotron radiation diffraction. This deformation method is used for obtaining structures with submicron and nanometer crystallite grain sizes. It has been revealed that the texture of the initial sample after the application of the ECAP method is characterized by two strong components (basic and prismatic), which form as a result of extrusion with back pressure. Under the deformation by the ECAP technology the basic component shifts by 45° relatively to the direction of the extrusion, which can be explained by the realization of the simple shear deformation mechanism.

II. Instrument development.

The work on the basic configuration of the new DN-6 diffractometer for studying microsamples on beam 6b of the IBR-2 reactor has been completed. The main elements of the diffractometer (mirror vacuum neutron guide, mechanical part, detector system) have been installed at beam 6b. First scientific and methodological experiments have been carried out and demonstrated a one-order increase in the neutron counting rate compared to that of the analogous DN-12 diffractometer.

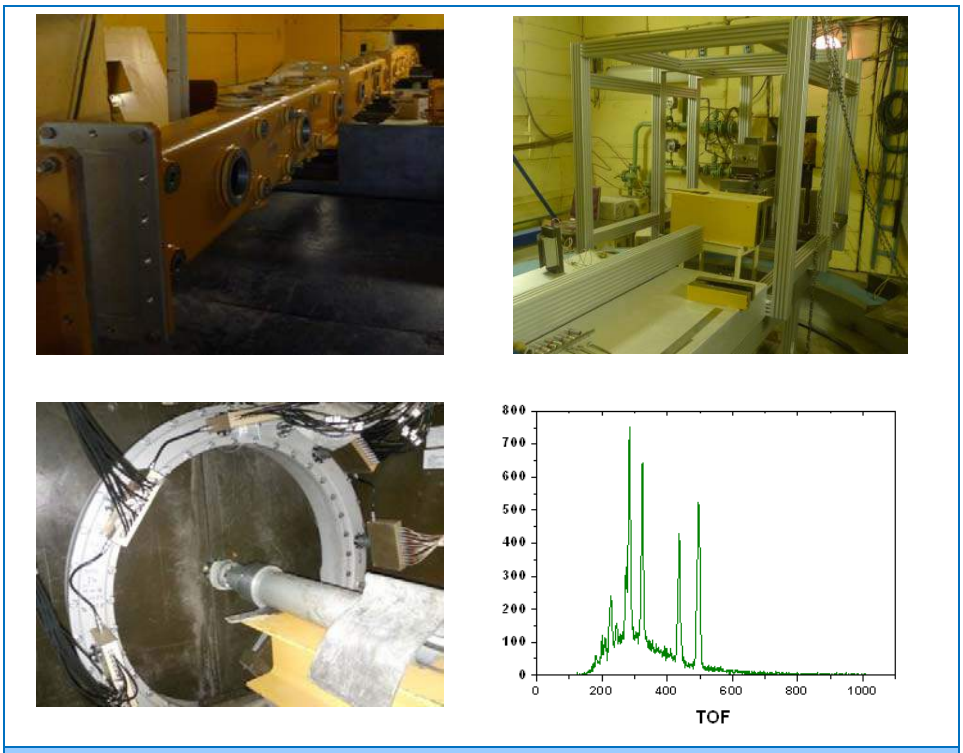

Fig. 14. Elements of the basic configuration of the DN-6 diffractometer: mirror vacuum neutron guide (top left), mechanical part (top right), detector system (bottom left), spectrum of a standard Ni sample (bottom right).

A large-scale modernization of the SKAT/Epsilon and NERA-PR diffractometers on beams 7a-1, 7a-2, 7-b (**Fig. 15**) aimed at the replacement of mirror neutron guides, installation of beam choppers and λ-choppers, modernization of the detector system, accumulation and sample environment electronics has been completed. On the NERA-PR spectrometer the integrated neutron flux at a sample position has approximately doubled and in the cold neutron range it has increased 4 times (in the operation mode with a cryogenic moderator). The analogous data for the SKAT/Epsilon are to be obtained. The instruments have been put into operation. A high pressure cell (Paris-Edinburgh type) has been purchased to extend experimental capabilities of the Epsilon diffractometer.

The work continued to construct a new multifunctional reflectometer GRAINS on beam 10 of the IBR-2M reactor. The improvement of the beam-forming system units has been carried out in order to eliminate the revealed design flaws. The final stage of the work on the design and construction of the reflectometer biological shielding has been completed. The electrical work necessary to prepare the spectrometer for commissioning is underway.

1. SCIENTIFIC RESEARCH

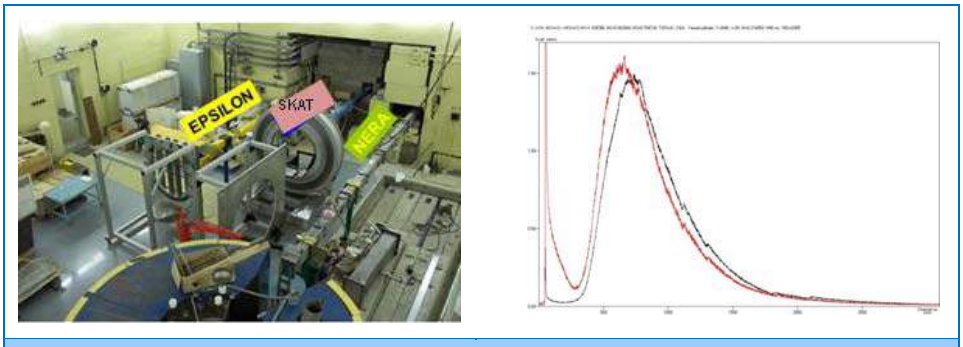

Fig. 15. Spectrometers SKAT, EPSILON and NERA on beams 7a-1, 7a-2 and 7b of the IBR-2M reactor (at the left). Incident neutron spectrum measured for a vanadium sample at the NERA-PR spectrometer before (black line) and after (red line) modernization – at the right.

The reconstruction of the DN-2 diffractometer into a diffractemeter for real-time measurements continued. A beam chopper, mirror neutron guide, 2D PSD with an active area of 200×200 mm^2 have been installed. First test measurements were started.

The final stage of the reconstruction of the head part of a neutron guide system for HRFD has been completed. A high vacuum in the new collimator-concentrator has been obtained. The development of algorithms and creation of the RTOF analyzer of a new type for registration of all events ("list mode") continued. A pilot prototype of the analyzer has been installed at FSD and the first experiments have been performed to compare the diffraction spectra obtained simultaneously using the existing DSP-based analyzer and the new "list mode" analyzer.

The re-adjustment of the elements of the REFLEX reflectometer has been carried out with due consideration for absolute measurements of neutron fluxes on beam 9 in 2011. The measurements have shown that the thermal neutron flux on beam 9 dropped significantly as compared with the parameters of 2006. The decrease in the neutron flux was induced by the change in the dimensions of the reactor core and the shift in the location of moderators relative to the axis of beam 9. To remedy the situation, all collimators of beam 9 were readjusted. The measurements of direct beam spectra conducted in May-June, 2012 showed the thermal neutron fluxes to be the same as it had been before the reactor shutdown in 2006. The adjustment and debugging of the electronics and software installed at the reflectometer at the end of 2011 went on through the year.

The creation of neutron beam infrastructure for the FSS diffractometer (moved from GKSS) and a prototype of a neutron radiography facility has started at beams 13 and 14 of IBR-2M. A biological shield has been built; the electrical work is nearing completion.

The measurements of the working parameters of the DIN-2PI spectrometer after the installation of a supermirror neutron concentrator have been completed. The gain factor estimated on the basis of the obtained results was found to be G (3 meV) ≈ 8.

A significant progress has been made in the development of neutron probe microscopy. The experiment was performed with a polarized neutron (4 Å) beam 2 μm wide formed by a layered waveguide, which was directed to an amorphous magnetic wire $(Co_{0.94}Fe_{0.06})_{72.5}Si_{12.5}B_{15}$ 190 μm in diameter with two types of magnetic domains (**Fig. 16**). As a result of scanning in the direction perpendicular to the neutron beam a cross sectional profile of a neutron spin precession angle was measured for the wire, thus making it possible to analyze its magnetic microstructure (distribution of magnetic induction). It has been experimentally demonstrated that statistically sufficient data on the

magnetic microstructure can be obtained for a reasonable measurement time (of the order of 10 hours).

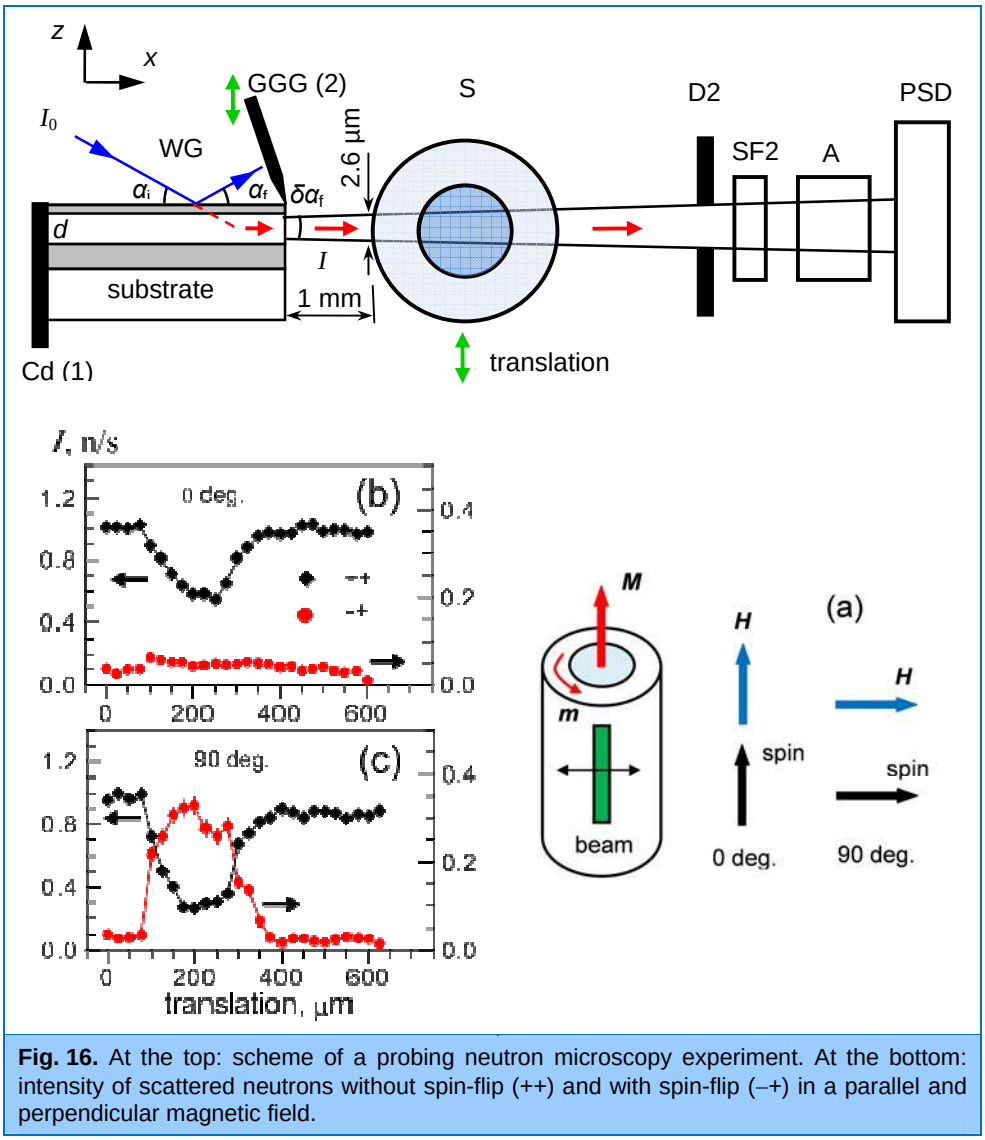

Fig. 16. At the top: scheme of a probing neutron microscopy experiment. At the bottom: intensity of scattered neutrons without spin-flip (++) and with spin-flip (–+) in a parallel and perpendicular magnetic field.

A theoretical problem of estimating the cross-section for thermal neutrons scattered by magnetic excitations in ferromagnetic layers several tens of nanometers thick has been considered. A method has been proposed to increase the cross-section by means of the resonant amplification of the neutron wave-function in a layered system with the optical potential of a special form. The scattering cross-section of neutrons with magnon absorption has been calculated taking into account the summation over all possible energy transfers depending on the scattering angle θ_S. It has been shown that at the sufficient neutron flux at the sample in the reflectometry experiment the observation of these processes is possible provided statistics are gathered during several days.

.

References

1. D.P. Kozlenko, A.F. Kusmartseva, E.V. Lukin, D.A. Keen, W.G. Marshall, M.A. de Vries and K.V. Kamenev, “From Quantum Disorder to Magnetic Order in an s=1/2 Kagome Lattice: A Structural and Magnetic Study of Herbertsmithite at High Pressure”, Phys. Rev. Lett. v. 108, pp. 187207 (1-5) (2012).
2. L. Melnikova, Z. Mitroova, M. Timko, J. Kovac, M .Koralewski, M. Pochylski, M.V. Avdeev, V.I. Petrenko, V.M. Garamus, L. Almasy, P. Kopcansky, Physical characterization of iron oxide nanoparticles in magnetoferritin, *Magnetohydrodynamics* (2012), accepted.
3. M.V. Avdeev, V.L. Aksenov, Z. Gažová, L. Almásy, V.I. Petrenko, H. Gojzewski, A.V. Feoktystov, K. Šipošová, A. Antošová, M. Timko, P. Kopčanský, On the determination of the helical structure parameters of amyloid protofilaments by small-angle neutron scattering and atomic-force microscopy, *J. Appl. Cryst.* (2012), accepted.
4. T.V. Tropin, N. Jargalan, M.V. Avdeev, O.A. Kyzyma, R.A. Eremin, D. Sangaa, V.L. Aksenov, Kinetics of cluster growth in polar solutions of fullerene: experimental and theoretical study of C_{60}/NMP solution, *J. Mol. Liq.* 175 (2012) 4-11.
5. R. Baddour-Hadjean, M.B. Smirnov, K.S. Smirnov, V. Kazimirov, J.M. Gallardo-Amores, U. Amador, M.E. Arroyo-de Dompablo, J.P. Pereira-Ramos, Lattice dynamics of β-V_2O_5: Raman spectroscopic insight into atomistic structure of a high pressure vanadium pentoxide polymorph. Chemistry of Materials, 51, 3194 (2012).
6. A.N. Nikitin, T. Lokajicek, A.A. Kruglov, R.N. Vasin, I.Yu. Zel’. Peculiarities of ultrasound propagation through layered structurally inhomogeneous solid bodies. Journal of Surface Investigation. X-ray, Synchrotron and Neutron Techniques. V.6, No.6, pp. 954-960 (2012).